Modeling the Normal Contact Characteristics between Components Joined in Multi-Bolted Systems

RAFAŁ GRZEJDA
Faculty of Mechanical Engineering and Mechatronics,
West Pomeranian University of Technology in Szczecin,
19 Piastow Ave., 70-310 Szczecin,
POLAND

Abstract: - This article is concerned with the modeling and calculation of the contact layer between components joined in a multi-bolted system for assembly conditions. The physical model of the multi-bolted connection is based on a system consisting of an elastic flange component, which is joined to an elastic support using a rigid-body bolt model. The contact layer between the joined components is described by a non-linear Winkler model. A model of the contact joint with consideration of the experimental normal elastic characteristics is presented. Examples of normal contact pressure distributions are included.

Key-Words: - contact joint, normal characteristics, multi-bolted system, preload, bolt-tightening sequence, finite element method.

Received: July 9, 2023. Revised: March 2, 2024. Accepted: April 11, 2024. Published: May 16, 2024.

1 Introduction

Multi-bolted systems are used for the mechanical fastening of components in all fields of engineering, particularly in mechanical or civil engineering, [1], [2], [3], [4], [5], [6], [7], [8], [9]. At present, they are more and more applied to join not only steel components, but also composite, [10], [11], [12] or additively manufactured components, [13], [14], [15]. There are even times when polylactic acid bolts manufactured by fused deposition modeling are used, [16]. Multi-bolted systems are therefore one of the most common detachable connections used in engineering practice.

In practice, multi-bolted connections used in preloaded systems are particularly important, [17], [18], [19], [20], [21], [22]. With a properly conducted preloading process, it is possible to prevent both self-loosening of the connection, [23], [24] and the phenomenon of connection unsealing, [25]. In addition, the gradual tightening of bolts during the assembly process, [26], [27], [28], [29] and the subsequent loading of preloaded systems with the working force, [30], [31] is equivalent to a variable contact layer pressure between the joined components. Hence, work on modeling the contact layer between the components of such connections is much needed.

Currently, finite element systems, [32], [33], [34], [35] are often applied in the modeling of contact joints in multi-bolted systems. Nevertheless, unfortunately, using the standard contact elements available in these systems, only constant stiffness coefficients for each contact element at the contact surface can be considered. In articles [31] and [36], numerical analyzes were carried out to determine the contact pressure at the interface between a serrated or flat gasket and a flange in a pipe connection. They used TARGET 170 and CONTA 174 contact elements available in ANSYS software with standard settings. The same type of finite elements and the same method for modeling contact joints were used in [33], [37], [38], [39], [40] among others. Authors using another popular commercial FEM software, ABAQUS, often assume contact properties as 'hard' contact in the normal direction without friction [41] or with friction, [42], [43], [44]. The same is true for another FEM software, Midas NFX. In this case, also, constant normal and tangential stiffness coefficients and a friction coefficient are inserted, [45]. In some works, the stiffness of the contact layer is not mentioned in detail in the modeling. It is then stated that the contact has been modelled in a standard way in the relevant software, [46], [47], [48].

In more advanced research, for example in [49], [50], [51], the contact layer between the components to be bolted together is replaced by a so-called virtual material, with which the features of the rough surfaces in contact are defined. Such features can be determined in experimental tests and can be

specified using the mechanical characteristics of the contact.

In the contact analysis of components joined in a multi-bolted system with experimentally defined characteristics, it is essential to take into account changes in the stiffness coefficients for each contact layer element. In such a case, further specific computational procedures are required and implemented in conjunction with the calculations performed in the finite element system.

Model tests of preload variation in multi-bolted connections can be validated by experimentally monitoring the forces in the bolts. Methods used in this regard are presented in [52], [53], [54] among others.

2 Model of the Multi-Bolted System

The general structure of the multi-bolted system is shown in Figure 1. The model consists of a pair of flexible components joined by bolts. A non-linear contact layer is introduced between the joined components. These four parts of the connection are regarded as subsystems of the multi-bolted system. The subsystems are denoted by symbols according to the following list:

- B – subsystem of bolts;
- F – joined component of the flange type;
- C – conventional non-linear contact layer;
- S – joined component of the support type.

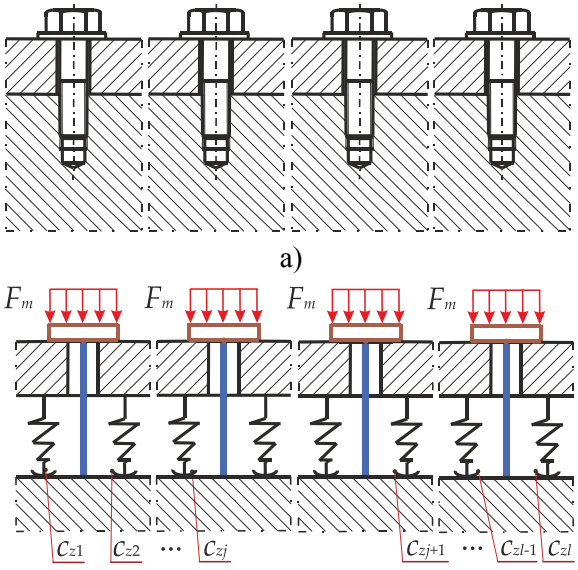

Fig. 1: Multi-bolted system: a) scheme, b) model of the system

By adopting the finite element method as the modeling method, the system components (flange and support) can be modeled using spatial finite elements. Bolts, on the other hand, can be modeled using a wide variety of models, including bar, beam, and spatial models.

The non-linear contact layer between joined components is modeled as a Winkler model, which is defined by a set of j (j = 1, 2, ..., l) one-sided springs, described by the following relation:

$$R_j = A_j \cdot f(u_{nj}) \tag{1}$$

where: R_j – force in the center of the j-th elementary contact area, A_j – j-th elementary contact area, u_{nj} – normal deformation of the j-th non-linear spring, respectively (for a review, see Figure 1).

The creation of the contact layer model proceeds in the following steps:

1. Dividing the contact area between the joined components (Figure 2a) into elementary contact areas (Figure 2b).
2. Addition of mesh nodes at the centers of gravity of the elementary contact areas (Figure 2b).
3. Insertion of non-linear springs at the nodes identified in the previous step.
4. Creation of a 2D finite element mesh on the contact area (Figure 2c).

Based on the 2D finite element mesh, a homogeneous 3D finite element mesh is generated at the interface between the joined components for the entire volume of the joined components.

The equilibrium equation of the system for the whole multi-bolted system can be written in the form:

$$\boldsymbol{K} \cdot \boldsymbol{q} = \boldsymbol{p} \tag{2}$$

where: $\boldsymbol{K}$ – stiffness matrix, $\boldsymbol{q}$ – vector of displacements, $\boldsymbol{p}$ – vector of loads, respectively.

Given the above division of the system into subsystems, Eq. (2) can be presented as:

$$\begin{bmatrix} \boldsymbol{K}_B & \boldsymbol{K}_{BF} & \boldsymbol{0} & \boldsymbol{K}_{BS} \\ \boldsymbol{K}_{FB} & \boldsymbol{K}_F & \boldsymbol{K}_{FC} & \boldsymbol{0} \\ \boldsymbol{0} & \boldsymbol{K}_{CF} & \boldsymbol{K}_C & \boldsymbol{K}_{CS} \\ \boldsymbol{K}_{SB} & \boldsymbol{0} & \boldsymbol{K}_{SC} & \boldsymbol{K}_S \end{bmatrix} \cdot \begin{bmatrix} \boldsymbol{q}_B \\ \boldsymbol{q}_F \\ \boldsymbol{q}_C \\ \boldsymbol{q}_S \end{bmatrix} = \begin{bmatrix} \boldsymbol{p}_B \\ \boldsymbol{p}_F \\ \boldsymbol{p}_C \\ \boldsymbol{p}_S \end{bmatrix} \tag{3}$$

where: $\boldsymbol{K_a}$ – stiffness matrix of the a-th subsystem, $\boldsymbol{K_{ab}}$ – matrix of elastic couplings between the a-th and b-th subsystems, $\boldsymbol{q_a}$ – vector of displacements of the a-th subsystem, $\boldsymbol{p_a}$ – vector of loads of the a-th subsystem, respectively, (a, b – symbols of the subsystems, $a \in \{B, F, C, S\}$, $b \in \{B, F, C, S\}$).

By solving the system of equations, a columnar displacement vector $\boldsymbol{q_C}$ is obtained:

$$\boldsymbol{q_C} = col(u_{n1}, u_{n2}, \ldots, u_{nj}, \ldots, u_{nl}) \tag{4}$$

In the next step, the forces R_j can be determined by Eq. (1).

The solution of Eq. (3) is carried out in an iterative process using the secant method, [55]. For the tightening of the first bolt, the linearization follows the method shown in Figure 3a, starting from the origin of the coordinate system. On the other hand, in the case of tightening the next bolt, it starts from the operating points W_j corresponding to the preload of the j-th non-linear spring in the previous calculation step (Figure 3b).

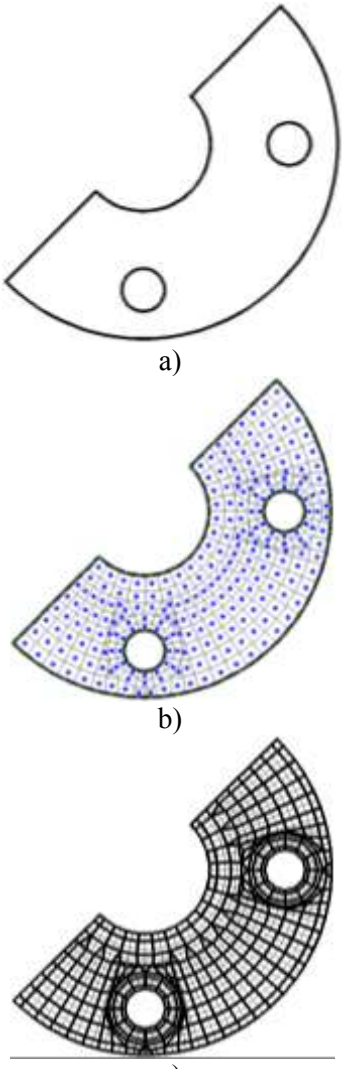

Fig. 2: Creating the finite element mesh at the contact surface between the joined components: a) real contact area, b) elementary contact areas, c) scheme of the mesh

At each tightening stage of the multi-bolted system, the linearization process is carried out until the following condition is met:

$$\left|\frac{R_c'-R_c}{R_c}\right| \leq \alpha \qquad (5)$$

where: R'_c – reaction in the j-th non-linear spring obtained from the linearization, R_c – actual reaction in the j-th non-linear spring, c – index dependent on the case of the calculation process ($c \in \{j, mj\}$), α – permissible linearization error, respectively.

Based on the obtained values of the normal deformation of the j-th non-linear spring u_{nj}, the normal contact pressure p_j on the j-th elementary contact surface can be determined according to the relation:

$$p_j = \frac{c_{zj} \cdot u_{nj}}{A_j} \qquad (6)$$

where: c_{zj} — stiffness coefficient of the j-th spring model (for a review, see Figure 1b).

As the next bolt to be tightened, the bolt lying in the area of the lowest mean normal pressure on the contact surface of the joined components is selected.

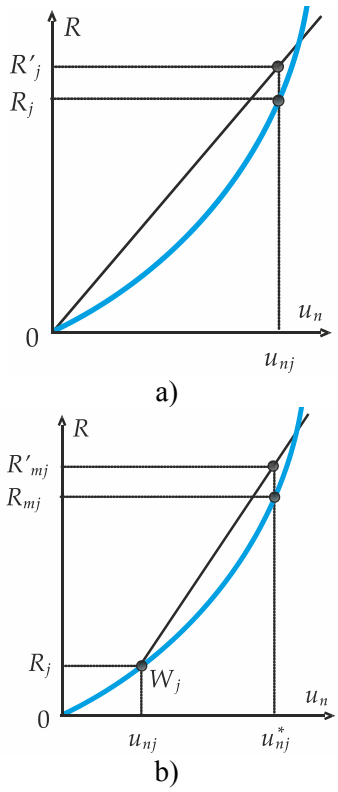

Fig. 3: Linearization of a curve by the secant method: a) in the case of the first bolt tightening, b) in the case of the next bolt tightening

3 Numerical Example

According to the presented method, the multi-bolted system shown in Figure 4a was calculated.

The calculations were carried out using the Midas NFX 2023 R1 software, [56]. A rigid body bolt model was used as the bolt model, [57], [58],

[59]. In contrast, the components were modeled using spatial elements, and the contact layer using non-linear spring models. The connection was fixed with seven M10 bolts. The calculations were performed for a thickness of the connected components h equal to 20 mm and a bolt preload F_{mi} equal to 20 kN. The optimal bolt-tightening sequence determined for the adopted multi-bolted system is set out in Table 1. This sequence is similar to a standard star pattern, [60], [61].

a) b)

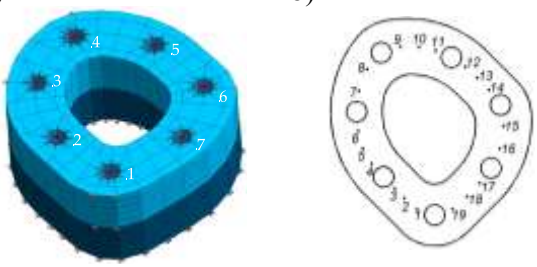

Fig. 4: FEM-based model of a multi-bolted system: a) adopted bolt numbering, b) nodes adopted to describe the distribution of normal contact pressure

Table 1. The optimal bolt-tightening sequence

Tightening Sequence	1	2	3	4	5	6	7
Bolt number	1	4	6	2	5	7	3

The stiffness characteristics of the springs lying in the contact layer were described by the following experimentally determined function, [18]:

$$R_j = A_j \cdot \left(3.428 \cdot {u_{nj}}^{1.657}\right) \tag{7}$$

whereby the quantities occurring in this formula are analogous to those in Eq. (1).

The numbering of the nodes used to describe the normal contact pressure distribution is shown in Figure 4b. The distribution of the normal contact pressure on the component surfaces along the line connecting the nodes indicated in Figure 4b, during the preloading process of the system, is shown in Figure 5.

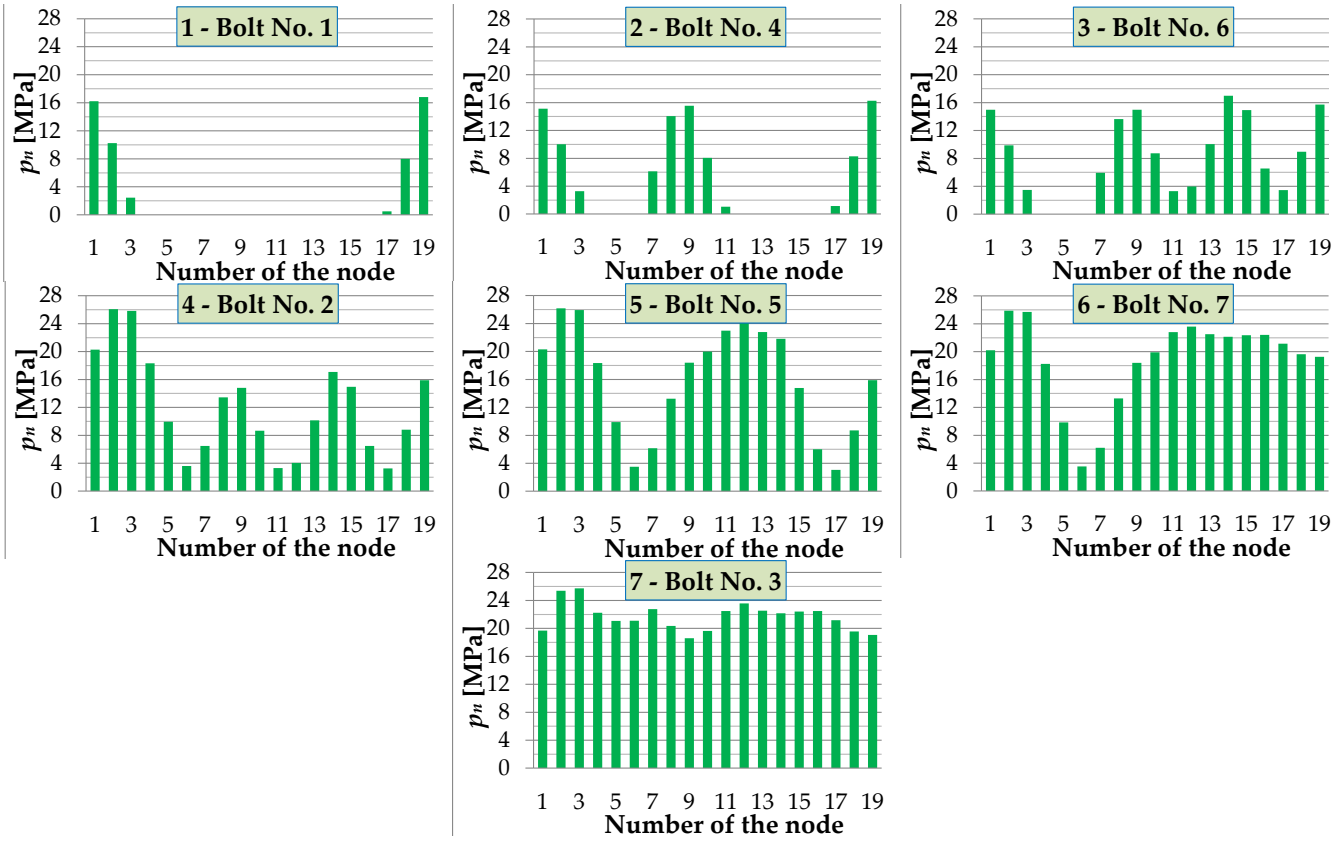

Fig. 5: Diagrams of normal pressure during the preload process for individual bolts in the system

An assessment of the final normal pressure values can be made using the *N*-index:

$$N = \frac{p_n - p_{an}}{p_{an}} \cdot 100\% \quad (8)$$

where: p_n — the value of the normal contact pressure on the *n*-th contact surface, associated with the *n*-th node (Figure 4b, n = 1, 2, …, 19); p_{an} — mean value of the normal contact pressure on the line joining the nodes shown in Figure 4b, respectively.

The values of the *N*-index range from -14.3 to 18.6%. This fact indicates a large variation in the value of the normal contact pressure on the analyzed surface of the joined components compared to their average value. Authors of such articles as [62], [63], [64], among others, came to similar conclusions based on studies of the preload process of various multi-bolted connections.

4 Conclusion

The presented model of a multi-bolted system can be effectively used in the analysis of bolt preload variation, once it has been prepared using CAx techniques, [65], [66]. Its implementation allows the control of the current value of the normal contact pressure between joined components and enables the selection of the optimal bolt-tightening sequence, which is particularly important for thin-walled structures used in aviation, [67], [68]. It is planned to further develop the model to take into account the operating condition of the multi-bolted system.

References:

[1] P. Zmarzły, Influence of the internal clearance of ball bearings on the vibration level, *Proceedings of the 24th International Conference Engineering Mechanics 2018*, Svratka, Czech Republic, 14-17 May 2018, pp. 961-964, https://doi.org/10.21495/91-8-961.

[2] P. Gutowski, M. Leus, Computational model of friction force reduction at arbitrary direction of tangential vibrations and its experimental verification, *Tribology International*, Vol. 143, 2020, Paper No. 106065, https://doi.org/10.1016/j.triboint.2019.106065.

[3] P. Zmarzły, Influence of bearing raceway surface topography on the level of generated vibration as an example of operational heredity, *Indian Journal of Engineering & Materials Sciences*, Vol. 27, No. 2, 2020, pp. 356-364, https://doi.org/10.56042/ijems.v27i2.45967.

[4] P. Zmarzły, Multi-dimensional mathematical wear models of vibration generated by rolling ball bearings made of AISI 52100 bearing steel, *Materials*, Vol. 13, No. 23, 2020, Paper No. 5440, https://doi.org/10.3390/ma13235440.

[5] T. Nakahara, M. Hirohata, S. Kondo, T. Furuichi, Paint coating removal by heating for high-strength bolted joints in steel bridge and its influence on bolt axial force, *Applied Mechanics*, Vol. 2, No. 4, 2021, pp. 728-738, https://doi.org/10.3390/applmech2040042.

[6] Ø. Karlsen, H. G. Lemu, I. Berkani, An investigation of the effects and consequences of combining expanding dual pin with radial spherical plain bearings, *Applied Mechanics*, Vol. 3, No. 2, 2022, pp. 573-589, https://doi.org/10.3390/applmech3020034.

[7] M. Nowakowski, J. Kurylo, Usability of perception sensors to determine the obstacles of unmanned ground vehicles operating in off-road environments, *Applied Sciences*, Vol. 13, No. 8, 2023, Paper No. 4892, https://doi.org/10.3390/app13084892.

[8] M. Leus, P. Gutowski, M. Rybkiewicz, Effectiveness of friction force reduction in sliding motion depending on the frequency of longitudinal tangential vibrations, sliding velocity and normal pressure, *Acta Mechanica et Automatica*, Vol. 17, No. 4, 2023, pp. 490-498, https://doi.org/10.2478/ama-2023-0057.

[9] M. Nowakowski, Perception technology for conversion of off-road vehicles for the purposes of unmanned missions, *Journal of Civil Engineering and Transport*, Vol. 5, No. 4, 2023, pp. 15-27, https://doi.org/10.24136/tren.2023.014.

[10] A. Prusinowski, R. Kaczyński, Investigation of tribological and strength properties of ABS/CF fibrous composites formed in fused deposition modeling, *Journal of Friction and Wear*, Vol. 41, No. 4, 2020, pp. 318-325, https://doi.org/10.3103/S106836662004011X.

[11] P. Wysmulski, The effect of load eccentricity on the compressed CFRP Z-shaped columns in the weak post-critical state, *Composite Structures*, Vol. 301, 2022, Paper No. 116184, https://doi.org/10.1016/j.compstruct.2022.116184

[12] P. Wysmulski, Numerical and experimental study of crack propagation in the tensile composite plate with the open hole, *Advances*

in Science and Technology – Research Journal, Vol. 17, No. 4, 2023, pp. 249-261, https://doi.org/10.12913/22998624/169970.

[13] L. Śnieżek, K. Grzelak, J. Torzewski, J. Kluczyński, Study of the mechanical properties components made by SLM additive technology, *Proceedings of the 11th International Conference on Intelligent Technologies in Logistics and Mechatronics Systems*, Panevėžys, Lithuania, 28-29 April 2016, pp. 145-153.

[14] A. Zdobytskyi, M. Lobur, T. Klymkovych, R. Kaczynski, A. Vasiliev, Use of methods and technologies of additive production for optimization of parameters of designs, *IOP Conference Series: Materials Science and Engineering*, Vol. 1016, 2021, Paper No. 012019, https://doi.org/10.1088/1757-899X/1016/1/012019.

[15] T. Šančić, M. Brčić, D. Kotarski, A. Łukaszewicz, Experimental characterization of composite-printed materials for the production of multirotor UAV airframe parts, *Materials*, Vol. 16, No. 14, 2023, Paper No. 5060, https://doi.org/10.3390/ma16145060.

[16] M. Kukla, I. Sieracki, W. Maliga, J. Górecki, Compression strength of PLA bolts produced via FDM, *Materials*, Vol. 15, No. 24, 2022, Paper No. 8740, https://doi.org/10.3390/ma15248740.

[17] A. Žiliukas, M. Kukis, Pressure vessel with corrugated core numerical strength and experimental analysis, *Mechanika*, Vol. 19, No. 4, 2013, pp. 374-379, https://doi.org/10.5755/j01.mech.19.4.3204.

[18] R. Grzejda, Modelling nonlinear preloaded multi-bolted systems on the operational state, *Engineering Transactions*, Vol. 64, No. 4, 2016, pp. 525-531, https://doi.org/10.24423/engtrans.738.2016.

[19] R. Grzejda, Impact of nonlinearity of the contact layer between elements joined in a multi-bolted system on its preload, *International Journal of Applied Mechanics and Engineering*, Vol. 22, No. 4, 2017, pp. 921-930, https://doi.org/10.1515/ijame-2017-0059.

[20] Y. Li, Z. Zhu, C. Wen, K. Liu, Z. Luo, T. Long, Rub-impact dynamic analysis of a dual-rotor system with bolted joint structure: Theoretical and experimental investigations, *Mechanical Systems and Signal Processing*, Vol. 209, 2024, Paper No. 111144, https://doi.org/10.1016/j.ymssp.2024.111144.

[21] B. Shi, Z. Luo, L. Li, Y. Li, K. Sun, Joint degradation and its effect on rotor vibration characteristics considering bolt assembly process, *Mechanical Systems and Signal Processing*, Vol. 211, 2024, Paper No. 111208, https://doi.org/10.1016/j.ymssp.2024.111208.

[22] L. Collini, R. Garziera, A. Corvi, G. Cantarelli, Slip strength of COR-TEN and Zn-coated steel preloaded bolted joints, *Results in Engineering*, Vol. 22, 2024, Paper No. 102009, https://doi.org/10.1016/j.rineng.2024.102009.

[23] L. Zhu, J. Hong, X. Jiang, On controlling pre-load and estimating anti-loosening performance in threaded fasteners based on accurate contact modeling, *Tribology International*, Vol. 95, 2016, pp. 181-191, https://doi.org/10.1016/j.triboint.2015.11.006.

[24] J. Zhang, W. Li, J. Feng, R. Liao, Critical load determination for preventing rotational loosening in bolted joints under dynamic transverse loads, *Engineering Failure Analysis*, Vol. 160, 2024, Paper No. 108217, https://doi.org/10.1016/j.engfailanal.2024.108217

[25] M. Abid, A. Khan, D. H. Nash, M. Hussain, H. A. Wajid, Optimized bolt tightening strategies for gasketed flanged pipe joints of different sizes, *International Journal of Pressure Vessels and Piping*, Vol. 139-140, 2016, pp. 22-27, https://doi.org/10.1016/j.ijpvp.2016.02.022.

[26] S. Kumakura, K. Saito, Tightening sequence for bolted flange joint assembly, *Proceedings of the 2003 ASME Pressure Vessels and Piping Conference, Analysis of bolted joints*, Cleveland, USA, 20-24 July 2003, pp. 9-16, https://doi.org/10.1115/PVP2003-1867.

[27] T. Takaki, T. Fukuoka, Methodical guideline for bolt-up operation of pipe flange connections (A case using sheet gasket and spiral wound gasket), *Proceedings of the 2003 ASME Pressure Vessels and Piping Conference, Analysis of bolted joints*, Cleveland, USA, 20-24 July 2003, pp. 23-30, https://doi.org/10.1115/PVP2003-1869.

[28] M. Abid, D. H. Nash, Structural strength: Gasketed vs non-gasketed flange joint under bolt up and operating condition, *International Journal of Solids and Structures*, Vol. 43, No. 14-15, 2006, pp. 4616-4629, https://doi.org/10.1016/j.ijsolstr.2005.06.078.

[29] K. A. Khan, M. Abid, J. A. Chattha, Gasketed bolted flange joint's relaxation behaviour

under different bolt up strategy, *Proceedings of the Institution of Mechanical Engineers, Part E: Journal of Process Mechanical Engineering*, Vol. 223, No. 4, 2009, pp. 259-263, https://doi.org/10.1243/09544089JPME263.

[30] R. Grzejda, Modelling nonlinear multi-bolted connections: A case of operational condition, *Proceedings of the 15th International Scientific Conference 'Engineering for Rural Development 2016'*, Jelgava, Latvia, 25-27 May 2016, pp. 336-341.

[31] P. Jaszak, J. Skrzypacz, A. Borawski, R. Grzejda, Methodology of leakage prediction in gasketed flange joints at pipeline deformations, *Materials*, Vol. 15, No. 12, 2022, Paper No. 4354, https://doi.org/10.3390/ma15124354.

[32] M. Caliskan, Evaluation of bonded and bolted repair techniques with finite element method, *Materials & Design*, Vol. 27, No. 10, 2006, pp. 811-820, https://doi.org/10.1016/j.matdes.2006.01.024.

[33] G. Shi, Y. Shi, Y. Wang, M. A. Bradford, Numerical simulation of steel pretensioned bolted end-plate connections of different types and details, *Engineering Structures*, Vol. 30, No. 10, 2008, pp. 2677-2686, https://doi.org/10.1016/j.engstruct.2008.02.013.

[34] D. A. Nethercot, E. L. Salih, L. Gardner, Behaviour and design of stainless steel bolted connections, *Advances in Structural Engineering*, Vol. 14, No. 4, 2011, pp. 647-658, https://doi.org/10.1260/1369-4332.14.4.647.

[35] T. N. Chakherlou, M. J. Razavi, A. B. Aghdam, On the variation of clamping force in bolted double lap joints subjected to longitudinal loading: A numerical and experimental investigation, *Strain*, Vol. 48, No. 1, 2012, pp. 21-29, https://doi.org/10.1111/j.1475-1305.2010.00795.x.

[36] P. Jaszak, The elastic serrated gasket of the flange bolted joints, *International Journal of Pressure Vessels and Piping*, Vol. 176, 2019, Paper No. 103954, https://doi.org/10.1016/j.ijpvp.2019.103954.

[37] L. Yang, Y. Wang, J. Guan, Y. Zhang, Y. Shi, Bearing strength of stainless steel bolted connections, *Advances in Structural Engineering*, Vol. 18, No. 7, 2015, pp. 1051-1062, https://doi.org/10.1260/1369-4332.18.7.1051.

[38] J. Cao, Z. Zhang, Finite element analysis and mathematical characterization of contact pressure distribution in bolted joints, *Journal of Mechanical Science and Technology*, Vol. 33, No. 10, 2019, pp. 4715-4725, https://doi.org/10.1007/s12206-019-0913-x.

[39] H. Wang, Q. Wu, H. Qian, K. Han, F. Fan, Buckling behavior of a circular steel tube with a bolt-ball joint under installation eccentricity, *Engineering Structures*, Vol. 197, 2019, Paper No. 109407, https://doi.org/10.1016/j.engstruct.2019.109407.

[40] M. M. Nia, S. Moradi, Surrogate models for endplate beam-column connections with shape memory alloy bolts, *Journal of Constructional Steel Research*, Vol. 187, 2021, Paper No. 106929, https://doi.org/10.1016/j.jcsr.2021.106929.

[41] T. Sadowski, M. Kneć, P. Golewski, Experimental investigations and numerical modelling of steel adhesive joints reinforced by rivets, *International Journal of Adhesion and Adhesives*, Vol. 30, No. 5, 2010, pp. 338-346, https://doi.org/10.1016/j.ijadhadh.2009.11.004

[42] M. Chybiński, Ł. Polus, Experimental and numerical investigations of aluminium-timber composite beams with bolted connections, *Structures*, Vol. 34, 2021, pp. 1942-1960, https://doi.org/10.1016/j.istruc.2021.08.111.

[43] O. Mijatović, A. Borković, M. Guzijan-Dilber, Z. Mišković, R. Salatić, R. Mandić, V. Golubović-Bugarski, Experimental and numerical study of structural damping in a beam with bolted splice connection, *Thin-Walled Structures*, Vol. 186, 2023, Paper No. 110661, https://doi.org/10.1016/j.tws.2023.110661.

[44] K. Liang, Z. Wang, Z. Yin, P. Hao, Investigation on bearing capacity and fracture behaviour of the bolt in a flange connection considering multiple load cases, *Structures*, Vol. 62, 2024, Paper No. 106252, https://doi.org/10.1016/j.istruc.2024.106252.

[45] R. Grzejda, M. Warzecha, K. Urbanowicz, Determination of pretension in bolts for structural health monitoring of multi-bolted connection: FEM approach, *Lubricants*, Vol. 10, No. 5, 2022, Paper No. 75, https://doi.org/10.3390/lubricants10050075.

[46] I. J. Drygala, M. A. Polak, J. M. Dulinska, Vibration serviceability assessment of GFRP pedestrian bridges, *Engineering Structures*, Vol. 184, 2019, pp. 176-185, https://doi.org/10.1016/j.engstruct.2019.01.072.

[47] P. Wysmulski, Load eccentricity of compressed composite Z-columns in non-linear state, *Materials*, Vol. 15, No. 21, 2022, Paper No. 7631, https://doi.org/10.3390/ma15217631.

[48] P. Wysmulski, Non-linear analysis of the postbuckling behaviour of eccentrically compressed composite channel-section columns, *Composite Structures*, Vol. 305, 2023, Paper No. 116446, https://doi.org/10.1016/j.compstruct.2022.116446.

[49] Y. Zhao, C. Yang, L. Cai, W. Shi, Z. Liu, Surface contact stress-based nonlinear virtual material method for dynamic analysis of bolted joint of machine tool, *Precision Engineering*, Vol. 43, 2016, pp. 230-240, https://doi.org/10.1016/j.precisioneng.2015.08.002.

[50] Y. Yang, H. Cheng, B. Liang, D. Zhao, J. Hu, K. Zhang, A novel virtual material layer model for predicting natural frequencies of composite bolted joints, *Chinese Journal of Aeronautics*, Vol. 34, No. 8, 2021, pp. 101-111, https://doi.org/10.1016/j.cja.2020.05.028.

[51] Y. Li, Y. Wang, Z. Liu, X. Yang, C. Zhang, Y. Cheng, A combined theoretical and experimental study on contact creep-induced clamping force relaxation of bolted joints at ambient temperature, *Marine Structures*, Vol. 85, 2022, Paper No. 103263, https://doi.org/10.1016/j.marstruc.2022.103263

[52] T. Wang, G. Song, S. Liu, Y. Li, H. Xiao, Review of bolted connection monitoring, *International Journal of Distributed Sensor Networks*, Vol. 9, No. 12, 2013, Paper No. 871213, https://doi.org/10.1155/2013/871213.

[53] P. Nazarko, L. Ziemianski, Force identification in bolts of flange connections for structural health monitoring and failure prevention, *Procedia Structural Integrity*, Vol. 5, 2017, pp. 460-467, https://doi.org/10.1016/j.prostr.2017.07.142.

[54] S. M. Y. Nikravesh, M. Goudarzi, A review paper on looseness detection methods in bolted structures, *Latin American Journal of Solids and Structures*, Vol. 14, No. 12, 2017, pp. 2153-2176, https://doi.org/10.1590/1679-78254231.

[55] J. A. Ezquerro, M. A. Hernández-Verón, Á. A. Magreñán, A. Moysi, A procedure to obtain quadratic convergence from the secant method, *Journal of Computational and Applied Mathematics*, Vol. 448, 2024, Paper No. 115912, https://doi.org/10.1016/j.cam.2024.115912.

[56] Midas NFX Analysis Manual, [Online]. https://globalsupport.midasuser.com/helpdesk/KB/View/32637163-midas-nfx-manuals-and-tutorials (Accessed Date: February 29, 2024).

[57] J. Aguirrebeitia, M. Abasolo, R. Avilés, I. F. de Bustos, General static load-carrying capacity for the design and selection of four contact point slewing bearings: Finite element calculations and theoretical model validation, *Finite Elements in Analysis and Design*, Vol. 55, 2012, pp. 23-30, https://doi.org/10.1016/j.finel.2012.02.002.

[58] C. Hammami, E. Balmes, M. Guskov, Numerical design and test on an assembled structure of a bolted joint with viscoelastic damping, *Mechanical Systems and Signal Processing*, Vol. 70-71, 2016, pp. 714-724, https://doi.org/10.1016/j.ymssp.2015.06.031.

[59] I. Coria, I. Martín, A.-H. Bouzid, I. Heras, M. Abasolo, Efficient assembly of bolted joints under external loads using numerical FEM, *International Journal of Mechanical Sciences*, Vol. 142-143, 2018, pp. 575-582, https://doi.org/10.1016/j.ijmecsci.2018.05.022

[60] I. Coria, M. Abasolo, I. Olaskoaga, A. Etxezarreta, J. Aguirrebeitia, A new methodology for the optimization of bolt tightening sequences for ring type joints, *Ocean Engineering*, Vol. 129, 2017, pp. 441-450, https://doi.org/10.1016/j.oceaneng.2016.10.049

[61] N. R. Nelson, N. S. Prasad, A. S. Sekhar, Structural integrity and sealing behaviour of bolted flange joint: A state of art review, *International Journal of Pressure Vessels and Piping*, Vol. 204, 2023, Paper No. 104975, https://doi.org/10.1016/j.ijpvp.2023.104975.

[62] Y. Li, Z. Liu, Y. Wang, L. Cai, W. Xu, Research on preload of bolted joints tightening sequence-related relaxation considering elastic interaction between bolts, *Journal of Constructional Steel Research*, Vol. 160, 2019, pp. 45-53, https://doi.org/10.1016/j.jcsr.2019.01.016.

[63] J. Braithwaite, A. Mehmanparast, Analysis of tightening sequence effects on preload behaviour of offshore wind turbine M72 bolted connections, *Energies*, Vol. 12, No. 23, 2019, Paper No. 4406, https://doi.org/10.3390/en12234406.

[64] I. Coria, M. Abasolo, J. Aguirrebeitia, I. Heras, Study of bolt load scatter due to tightening sequence, *International Journal of Pressure Vessels and Piping*, Vol. 182, 2020, Paper No. 104054, https://doi.org/10.1016/j.ijpvp.2020.104054.

[65] A. Łukaszewicz, Modelling of solid part using multibody techniques in parametric CAD systems, *Solid State Phenomena*, Vol. 147-149, 2009, pp. 924-929, https://doi.org/10.4028/www.scientific.net/SSP.147-149.924.

[66] A. Łukaszewicz, K. Szafran, J. Józwik, CAx techniques used in UAV design process, *Proceedings of the 2020 IEEE 7th International Workshop on Metrology for AeroSpace (MetroAeroSpace)*, Pisa, Italy, 22-24 June 2020, pp. 95-98, https://doi.org/10.1109/MetroAeroSpace48742.2020.9160091.

[67] W. Grodzki, A. Łukaszewicz, Design and manufacture of umanned aerial vehicles (UAV) wing structure using composite materials, *Materials Science & Engineering Technology*, Vol. 46, No. 3, 2015, pp. 269-278, https://doi.org/10.1002/mawe.201500351.

[68] Y. N. Saravanakumar, M. T. H. Sultan, F. S. Shahar, W. Giernacki, A. Łukaszewicz, M. Nowakowski, A. Holovatyy, S. Stępień, Power sources for Unmanned Aerial Vehicles: A state-of-the art, *Applied Sciences*, Vol. 13, No. 21, 2023, Paper No. 11932, https://doi.org/10.3390/app132111932.

Contribution of Individual Authors to the Creation of a Scientific Article (Ghostwriting Policy)

The author contributed to the present research, at all stages from the formulation of the problem to the final findings and solution.

Sources of Funding for Research Presented in a Scientific Article or Scientific Article Itself

No funding was received for conducting this study.

Conflict of Interest

The author has no conflicts of interest to declare.